RSC Advances

This article can be cited before page numbers have been issued, to do this please use: N. Wang, Z. Han, H. Fan and S. Ai, *RSC Adv.*, 2015, DOI: 10.1039/C5RA18957H.

ROYAL SOCIETY OF CHEMISTRY

www.rsc.org/advances

View Article Online
DOI: 10.1039/C5RA18957H

Graphical Abstract

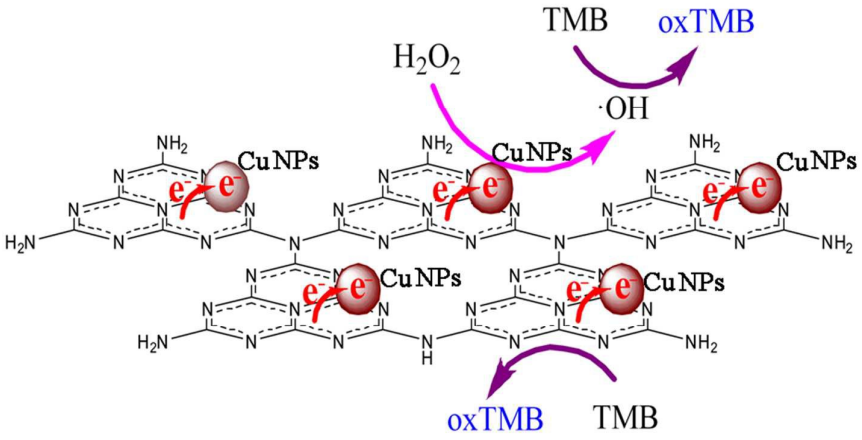

CuNPs/g-C_3N_4 was successfully prepared by the calcination of dicyandiamide-Cu^{2+} complex as peroxidase mimic for sensitive detection of glucose.

View Article Online
DOI: 10.1039/C5RA18957H

Journal Name

ARTICLE

Copper nanoparticles modified graphitic carbon nitride nanosheet as peroxidase mimetic for glucose detection

Received 00th January 20xx,
Accepted 00th January 20xx

DOI: 10.1039/x0xx00000x

www.rsc.org/

Nan Wang, Zhenwei Han, Hai Fan*, Shiyun Ai*

In this study, copper nanoparticles modified graphitic carbon nitride nanosheet (CuNPs/g-C_3N_4) as a novel peroxidase mimetic was successfully prepared by the calcination of dicyandiamide-Cu^{2+} complex with the assistance of humic acid. The morphology and structure of the product was characterized by X-ray powder diffractmeter (XRD), Fourier transform infrared spectroscopy (FTIR) and transmission electron microscopy (TEM). The prepared CuNPs/g-C_3N_4 was found to have highly peroxidase-like activity, which can rapidly catalyze the oxidation of peroxidase substance 3, 3′, 5, 5′-tetramethylbenzidine (TMB) to produce a blue color reaction in the presence of H_2O_2. Accordingly, a simple, selective and fast colorimetric method was developed for H_2O_2 and glucose detection. The prepared CuNPs/g-C_3N_4 exhibited low detection limits with 3.2×10^{-8} M and 3.7×10^{-7} M for H_2O_2 and glucose, respectively, due to the excellent peroxidase-like activity of Cu NPs/g-C_3N_4 originated from the synergistic effect of Cu NPs and g-C_3N_4. In this work, we utilized the easily forming complex ability of dicyandiamide and Cu^{2+} ions to form a homogeneous precursor solution, and then obtained CuNPs/g-C_3N_4 product, such method may have wide applications in novel composite nanomaterials preparation. The product may have promising applications in medical diagnostics and biotechnology fields.

1. Introduction

Since Fe_3O_4 magnetic nanoparticles were discovered to exhibit an intrinsic peroxidase-like activity for the first time [1], great interest has been focused on the nanoparticles as enzyme mimetics. Consequently, a variety of nanoparticles were found to have peroxidase- or oxidase-like activity [2, 3]. Among them, metal nanoparticles have attracted much attention due to their low toxicity, ultrafine size and high enzyme activity [4]. Several metal nanomaterials such as Au nanoparticles [5] and Pt nanoparticles [6] were discovered to exhibit a high intrinsic peroxidase-like enzyme mimetic activity. Consequently, bimetallic or hybrid nanomaterials such as Au@Pt nanostructures [7], CuPt nanorods [8], Bi-Au nanoparticles [9] and Au@Pd nanoparticles [10], have also been reported to have excellent peroxidase-like activity. However, these noble metals usually have high cost, which limited their practical applications.

Recently, Cu based nanomaterials have brought increasing attention due to their much lower cost compared to noble metals such as Au, Pt, Pd. Several methods, such as vapor depositions [11, 12], reverse micellar system [13, 14], soft and hard template processes [15, 16] and electrochemical reaction [17] have been developed for the synthesis of Cu nanocrystals. However, pure Cu nanocrystals are not stable in air, which is easily oxidized to form copper oxides. To solve this problem, stabilizing agents are necessary during the synthesized process. For example, Nirmal Goswami et al. reported extremely stable, water-soluble Cu quantum clusters by capped with bovine serum albumin [18]. However, the Cu NPs obtained by these methods are easily aggregated, which hindered their further applications. Therefore, it is necessary to provide facile synthetic route for synthesis of Cu NPs with good dispersity and stability.

Graphitic carbon nitride (g-C_3N_4) has become a hot research topic recently due to many advantages such as high thermal and chemical stability, tunable electronic structure, abundant and inexpensive raw materials [19]. Several potential applications have been developed, such as photocatalyst, bioimaging and biomedical applications [20-27]. Recently, g-C_3N_4 has also been found to have peroxidase-like activity. g-C_3N_4 has a stacked two-dimensional (2D) structure, which can be easily exfoliated into nanosheets. Nanosheets are regarded as ideal supports for the formation of functional composites. As we all know that the precursors for the preparation of g-C_3N_4 are usually amino groups contained compounds, such as dicyandiamide. These amino groups can interact with copper ions to form stable complex due to the strong coordination force between amino and copper ions. This inspired us to take advantage of dicyandiamide-Cu^{2+} complex as the precursor for the formation of carbon nitride and Cu composite with functional properties. During the formation of carbon nitride nanosheets, Cu NPs would be dispersed on nanosheets uniformly, which could largely enhance the catalytic activity and reduce the cost at the same time.

[a] College of Chemistry and Material Science, Shandong Agricultural University, Taian, 271018, Shandong, P. R. China. E-mail: fanhai@sdau.edu.cn; ashy@sdau.edu.cn; Fax: +86 538 8242251; Tel: +86 538 8247660

View Article Online
DOI: 10.1039/C5RA18957H

Herein, we report the formation of Cu NPs modified g-C_3N_4 nanosheet by calcination of dicyandiamide-Cu^{2+} complex with the reduction of humic acid. The prepared Cu NPs/g-C_3N_4 possesses intrinsic peroxidase-like activity, which have much better peroxidase-like activity than Cu NPs and g-C_3N_4 under the reaction of H_2O_2 and TMB. Accordingly, a novel colorimetric method for the detection of H_2O_2 and glucose was developed. Most importantly, this rapid, sensitive, and convenient approach could be applied for glucose detection in real serum samples, which can be potentially applied in biotechnology and medical diagnostics.

2. Experimental Section

2.1 Chemicals and reagents

Dicyandiamide, copper acetate, glucose oxidase and TMB were analytically pure and purchased from Aladdin (Shanghai, China). Humic acid, H_2O_2 and other chemical reagents were purchased from Kay Tong Chemical Reagents Co., Ltd (Tianjin, China). The blood samples were provided by the university hospital. All reagents were of analytical grade and used without further purification. Phosphate buffer solution (PBS, pH from 2.0 to 7.0) was used in this work and double distilled water was applied throughout the experiment.

2.2 Synthesis of the Cu NPs/g-C_3N_4

Firstly, dicyandiamide and copper acetate were mixed in the aqueous solution with stirring. Cu^{2+} ions were coordinated with dicyandiamide to form a dicyandiamide-Cu^{2+} complex due to the strong coordination interaction between Cu^{2+} ions and the amino groups on the dicyandiamide. Then the mixture was filtered and dried. Secondly, the obtained product and humic acid were grinded on the agate mortar and put into a porcelain crucible covered with a lid in a muffle fumace at 3 °C/min up to 550 °C for 2 hours in nitrogen atmosphere.

2.3 Characterization

The crystal structure and phase purities of as-synthesized products were characterized by X-ray powder diffractmeter (XRD). The XRD data was collected using a Rigaku DLMAX-2550V diffractmeter. Transmission electron microscopy (TEM) was performed on a JEM-2010 transmission electron microscope (Japan). Kinetic measurements and UV-Vis absorption spectra were carried out using a UV-2450 Shimadzu Vis-spectrometer. Photographs were taken using a Canon G11 digital camera.

2.4 The catalytic activity of Cu NPs/g-C_3N_4

The catalytic activity measurements of Cu NPs/g-C_3N_4 were performed in PBS buffer (25 mM, pH 4.0) containing Cu NPs/g-C_3N_4 samples (80 μL), in the presence of H_2O_2 (100 mM) and TMB (8 mM) at room temperature, unless otherwise stated. The assays were monitored in wavelength-scan mode after reacted for 10 min or time-course mode at 652 nm under the optimal conditions as described above, unless otherwise stated.

2.5 Detection of H_2O_2 and glucose using Cu NPs/g-C_3N_4 as peroxidase mimetic

Colorimetic detection of glucose based on Cu NPs/g-C_3N_4 as peroxidase mimetic was investigated. Michaelis-Menten constant (K_m) was obtained under the optimal conditions by varying the concentrations of H_2O_2 and TMB. K_m was calculated using Lineweaver-Burk plots of the double reciprocal of the Michaelis-Menten equation, $1/v = (K_m/V_{max})(1/[S]) + 1/V_{max}$. In this equation, v is the initial velocity, V_{max} is the maximal reaction velocity, and [S] is the concentration of the substrate.

H_2O_2 detection was carried out as follows: 80 μL Cu NPs/g-C_3N_4 (0.5 mg mL^{-1}), 40 μL TMB (8 mM) and 200 μL phosphate buffer (25 mM, pH 3.0) were mixed and incubated in 500 μL centrifugal tube. Then 80 μL H_2O_2 solutions with different concentrations were added. The mixed solution was further incubated at room temperature for 10 min. The absorbance of supernatant was recorded.

Glucose detection was realized as follows: 5 μL GOx (40 mg mL^{-1}) was added into 100 μL phosphate buffer (25 mM) containing different concentrations of glucose. Then the mixed solution was incubated at 37 °C for 1 h to produce H_2O_2. The other detection procedure was the same as that of H_2O_2.

The specificity of the Cu NPs/g-C_3N_4 for glucose was tested using 10 mM maltose, 10 mM fructose, 10 mM lactose, and 5 mM glucose. The detection procedure was the same as that of H_2O_2. Before the detection of glucose in blood samples, the blood samples were pretreated by salting-out and centrifugation to remove proteins. The supernatant solution was taken and diluted with phosphate buffer (25 mM). 100 μL of above solution was mixed with 5 μL GOx (40 mg mL^{-1}), and then the mixture was incubated at 37 °C for 1 h to produce H_2O_2. The other detection procedure was the same as that of H_2O_2.

3. Results and discussion

3.1 Characterization of the products

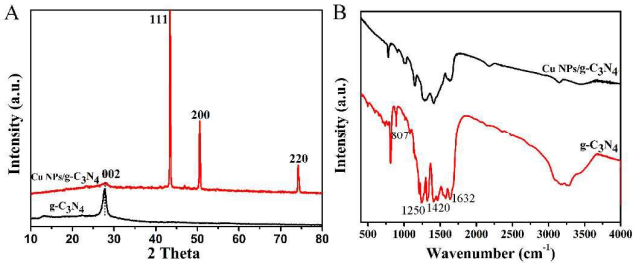

Fig. 1 (A) XRD patterns and (B) FTIR spectra of g-C_3N_4 and Cu NPs/g-C_3N_4.

The phase and structure of as-synthesized products were characterized by XRD and FTIR. In the XRD pattern (Fig. 1A), the apparent peak of 27.7° is assigned to the characteristic peak of g-C_3N_4 [28, 29]. To the red XRD pattern of the Cu NPs/g-C_3N_4, besides the C_3N_4 diffraction peak at 27.7°, all the other three peaks at 43.4°, 50.5° and 74.2° can be assigned to the (111), (200) and (220) crystal face of Cu (JCPDS No. 04-0836). No other diffraction peaks of impurities can be observed. It confirmed the successful preparation of pure Cu NPs/g-C_3N_4

View Article Online
DOI: 10.1039/C5RA18957H

nanocomposite. FTIR was further used to characterize the product, as shown in Fig. 1B. The peak at 807 cm^{-1} belongs to triazine ring mode, one typical peak in carbon nitride. The absorption bands near 1572 and 1632 cm^{-1} are attributed to C=N stretching, while the bands at 1250, 1325, 1420 cm^{-1} are consistent with aromatic C-N stretching. The broad band at 3000-3500 cm^{-1} appears for uncondensed terminal amino groups (-NH_2 or = NH groups). To Cu NPs/g-C_3N_4 nanocomposite, all absorption peak positions in the case of Cu NPs/g-C_3N_4 are almost similar to those in the case of g-C_3N_4, which indicates that the structure of g-C_3N_4 keeps almost the same with that after addition of Cu NPs [29].

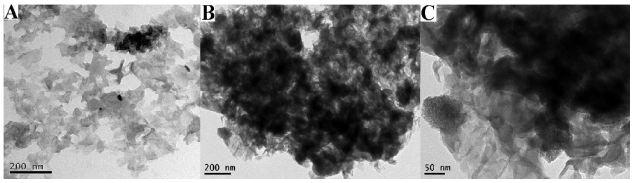

Fig. 2 TEM images: (A) g-C_3N_4, (B) and (C) Cu NPs/g-C_3N_4 with different magnification.

The morphology of the Cu NPs/g-C_3N_4 nanocomposite is investigated by TEM. In Fig. 2A, g-C_3N_4 nanosheet can be obviously observed. Fig. 2B showed that Cu NPs are uniformly dispersed on the surface of g-C_3N_4 nanosheets, forming the assembly of g-C_3N_4 nanosheets and Cu spherical nanostructures. From the magnification image in Fig. 2C, it can be clearly observed that each Cu spherical nanostructure is composed of many little Cu nanoparticles. Such special morphology may be due to the viscosity of humic acid besides its reduction property. The characterization results suggest that Cu NPs/g-C_3N_4 has been successfully synthesized.

3.2 Peroxidase-like activity of Cu NPs/g-C_3N_4

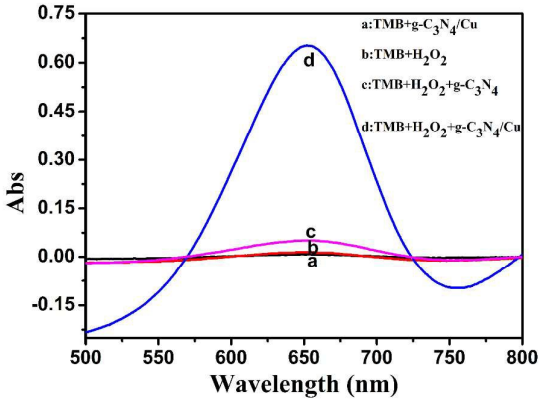

Fig. 3 Absorbance spectra of TMB (800 μM) in different reaction systems. Solutions in 25 mM PBS (pH 3.0) incubated at the room temperature for 10 min.

In this study, catalytic oxidation of the typical peroxidase substrate TMB in the different systems was conducted to demonstrate the peroxidase-like activity of as-synthesized Cu NPs/g-C_3N_4. In Fig. 3, the TMB + Cu NPs/g-C_3N_4 system without H_2O_2 results in a very slight absorbance at 652 nm. And the H_2O_2 + TMB system without any g-C_3N_4 or Cu NPs/g-C_3N_4 samples shows an ignorable absorbance. However, the H_2O_2 + TMB + g-C_3N_4 system has an absorbance at 652 nm indicating the production of oxidized TMB. And thus proves that the g-C_3N_4 owns intrinsic peroxidase-like activity. The H_2O_2 + TMB + Cu NPs/g-C_3N_4 system has a strongest absorbance at 652 nm, demonstrating the high catalytic efficiency and the excellent peroxidase-like activity of Cu NPs/g-C_3N_4. The excellent activity is due to the Cu nanoparticles dispersed on the C_3N_4 nanosheets, which produces the synergistic enhanced catalytic activity effect.

3.3 Optimization of reaction conditions

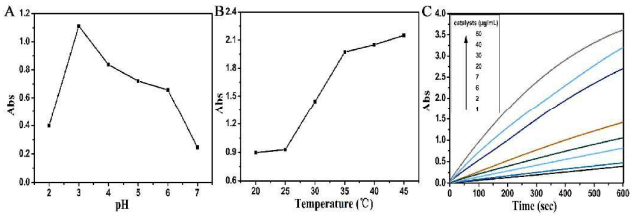

Fig. 4 Dependence of peroxidase-like activity of Cu NPs/g-C_3N_4 on (A) pH, (B) temperature and (C) concentration of Cu NPs/g-C_3N_4. Experiments were carried out using Cu NPs/g-C_3N_4 in 25 mM PBS (pH 3.0) solution with 10 mM H_2O_2 and 800 μM TMB as substrates.

To explore the optimal reaction conditions, influence of pH and temperature on the catalytic activity of Cu NPs/g-C_3N_4 was studied. When the pH of phosphate buffer varied from 2.0 to 7.0, the activity of Cu NPs/g-C_3N_4 was investigated as shown in Fig. 4A. It was found that the peak intensity increases first and then decrease with the pH varying from 2.0 to 7.0. At pH 3.0, the absorption intensity becomes the maximum. Therefore, the optimal pH value is pH 3.0. The temperature ranging from 20 °C to 45 °C was also performed in this experiment. As shown in Fig. 4B, the absorbance at 652 nm increased obviously initially but much more slowly after 35 °C. Thus, 35 °C is selected during the experiment. In addition, the concentration of Cu NPs/g-C_3N_4 also has an influence on the catalytic reaction. Fig. 4C shows the time-dependent absorbance changes of TMB solution with addition different concentration of Cu NPs/g-C_3N_4 in 25 mM PBS (pH 3.0) at room temperature. With the concentration of Cu NPs/g-C_3N_4 increased, the reaction rate increased correspondingly. 50 $\mu g \cdot mL^{-1}$ was used in our following experiment.

In order to study the catalytic mechanism, steady-state kinetics with H_2O_2 or TMB as substrate was measured by changing the concentration of one substrate while the other conditions kept constant. Typical Michaelis-Menten curves could be acquired for both TMB and H_2O_2 in a range of concentrations of one substrate as shown in Fig. 5A and B. The double reciprocal plots were obtained according to the calculated series of the initial reaction rates. In Fig. 5C, every straight line was obtained by changing reciprocal initial velocity with reciprocal TMB concentration keeping H_2O_2 concentration constant. Three approximate parallel lines were obtained by varying the concentration of H_2O_2. Similarly, reciprocal initial velocity versus reciprocal H_2O_2 concentration was collected by varying concentration of TMB as shown in Fig.

View Article Online
DOI: 10.1039/C5RA18957H

5D. The results show that the slopes of the plots are almost parallel, which should be the characteristic of a ping-pong mechanism. Moreover, Lineweaver-Burk plot was used to calculate Michaelis-Menten constant (K_m) and maximal reaction velocity (V_{max}) in this system. The calculated values are recorded in table 1. The Km values indicate the affinity for the structure. The Km value for the Cu NPs/g-C_3N_4 was 0.389 mM, which is much lower than that of AuNPs/PVP-GNs (2.63 mM) [30]. The result indicated that the Cu NPs/g-C_3N_4 have a significantly high affinity.

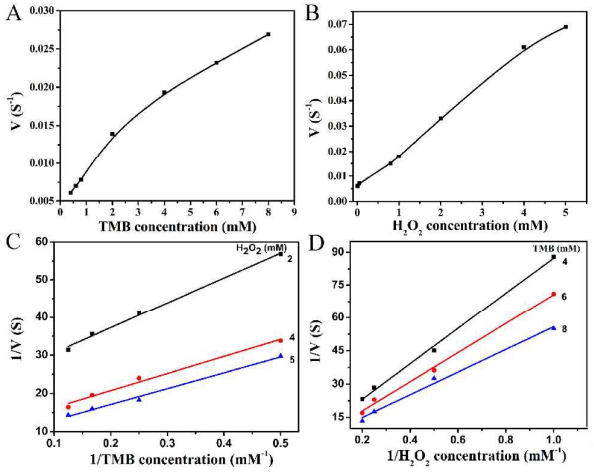

Fig. 5 Steady-state kinetic assay and catalytic mechanism of Cu NPs/g-C_3N_4. (A) The concentration of H_2O_2 was 4 mM and TMB concentration was varied. (B) The concentration of TMB was 8 mM and H_2O_2 concentration was varied. (C and D) Double reciprocal plots of activity of Cu NPs/g-C_3N_4 with the concentration of one substrate (H_2O_2 or TMB) fixed and the other varied. The velocity (v) of the reaction was measured using 0.15 mg·mL^{-1} Cu NPs/g-C_3N_4 in 400 μL of 25 mM PBS (pH 3.0) at room temperature.

Table 1 The Michaelis-Menten constant (K_m) and maximum reaction rate (V_{max}) of Cu NPs/g-C_3N_4.

catalyst	substance	K_m [mM]	V_{max} (10^{-7} M s^{-1})
Cu NPs/g-C_3N_4	TMB	0.389	5.84
Cu NPs/g-C_3N_4	H_2O_2	9.27	3.84

3.4 Detection of H_2O_2 and glucose

According to the excellent peroxidase-like activity of our prepared Cu NPs/g-C_3N_4, the colorimetric method for detection of H_2O_2 and glucose using Cu NPs/g-C_3N_4-catalyzed blue color reaction was developed. The catalytic activity of Cu NPs/g-C_3N_4 is H_2O_2-concentration-dependent and thus can be used to detect H_2O_2. Fig. 6A shows the typical H_2O_2 concentration-response curve under the optimal conditions (pH 3.0, 35 °C). In Fig. 6B, the linear calibration plot ranges from 1.0×10^{-7} to 2.0×10^{-6} M. The detection limit is calculated to be H_2O_2 is 3.2×10^{-8} M. Because, H_2O_2 is the main product of glucose oxidation in the presence of O_2 while catalyzed by glucose oxidase, therefore, the detection of glucose can also be realized according the quantitative relationship between glucose and H_2O_2. In Fig. 6C, the typical glucose concentration-response curve exhibits that glucose can be visually determined. In Fig. 6D, the linear range of glucose detection is from 1.0×10^{-6} to 1.0×10^{-4} M with a detection limit of 3.7×10^{-7} M. The detection limits of our prepared Cu NPs/g-C_3N_4 are much lower than those in most of the reported literatures, as shown in table 2.

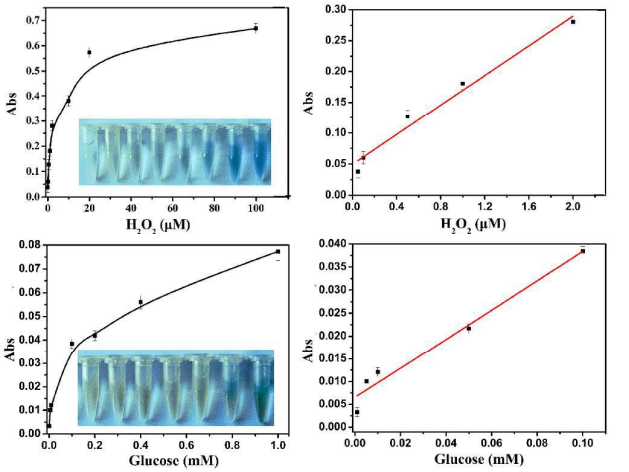

Fig. 6 (A) Absorbance changes at 652 nm of TMB solutions catalyzed by Cu NPs/g-C_3N_4 in the presence of different concentrations of H_2O_2 in 25 mM PBS (pH 3.0) at room temperature. (B) A dose-response curve for H_2O_2 detection. (C) Absorbance changes at 652 nm of TMB reaction solutions catalyzed by Cu NPs/g-C_3N_4 in the presence of different concentrations of glucose in 25 mM PBS (pH 3.0) at room temperature. (D) A dose-response curve for glucose detection. Insert: photos of the solution during and after the detection of H_2O_2 and glucose.

Table 2 The comparisons of detection limits using different materials as peroxidase mimetics for H_2O_2/glucose detection.

Materials	Methods	H_2O_2/glucose	Detection limit	Reference
Cu NPs/g-C_3N_4	colorimetric	H_2O_2 glucose	0.032 μM 0.37 μM	/
g-C_3N_4	colorimetric	H_2O_2 glucose	5 μM 1 μM	31
Cu NCs	colorimetric	H_2O_2 glucose	10 μM 100 μM	32
Pt NTs	colorimetric	H_2O_2 glucose	18.6 μM /	6
Fe-g-C_3N_4	colorimetric	H_2O_2 glucose	0.05 μM 0.5 μM	33

It is interesting to note that the detection sensitivity of our prepared Cu NPs/g-C_3N_4 for the detection of H_2O_2 and glucose is not only much higher than those of g-C_3N_4 [31] and Cu NCs [32], but higher than those of many reported peroxidase mimetics. Such unusual high detection performance probably originated from the synergistic effect of Cu NPs and g-C_3N_4, as shown in scheme 1. Firstly, g-C_3N_4 nanaosheets provide an ideal platform for the high dispersion of Cu NPs. Secondly, g-C_3N_4 nanosheets have π-conjugated electronic structure. The electrons would transfer from g-C_3N_4 nanosheets to Cu NPs

View Article Online
DOI: 10.1039/C5RA18957H

due to the low Fermi level of metals [34]. More electrons would catalylize more H_2O_2 to ·OH by giving electrons to H_2O_2. Herein, the existence of Cu NPs accelerates the electron transfer rate from C_3N_4 to H_2O_2. Therefore, our prepared Cu NPs/g-C_3N_4 demonstrates much higher catalytic activity.

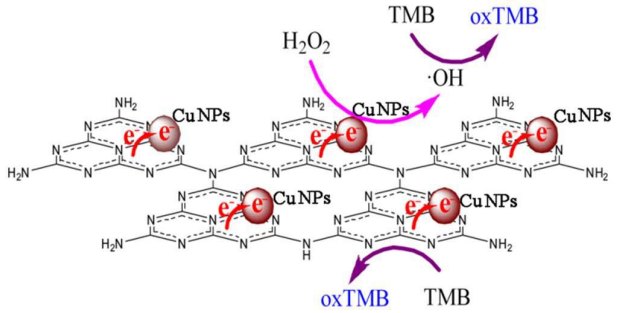

Scheme 1 The enhanced catalytic mechanism of Cu NPs/g-C_3N_4.

In order to test the selectivity of the colorimetric method for glucose, 10 mM fructose, 10 mM lactose, and 10 mM maltose were selected as the control samples. Fig. 7A shows the absorption intensity of solution in the presence of glucose or other analogues. To glucose, the absorption intensity is much higher than that of other analogues, even though the concentrations of analogues were 2 times higher than that of glucose. The main reason is that glucose oxidase has a certain degree of specificity to glucose, so the absorbance hardly increased for analogues as shown in Fig. 7A. Therefore, the colorimetric method proposed in our experiment is a simple, speed, and selective colorimetric method for the detection of glucose. To test the application of this method on real samples, blood sample was selected to detect glucose. Fig. 7B shows the time-dependent absorbance changes of solutions in the absence or presence of samples. According to the linear calibration curve, glucose in the blood sample can be calculated to be 7.12 mM. The error is minimal for the provided value of 6.85 mM from the hospital. In addition, the normal range of blood glucose concentration in healthy is about 3-8 mM. Therefore, this colorimetric method can be conveniently applied to glucose detection.

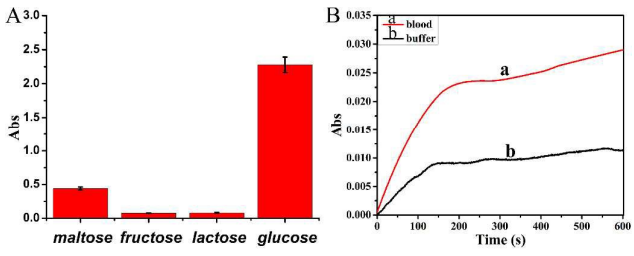

Fig. 7 (A) Selectivity analysis for glucose detection by monitoring the relative absorption intensity. The analyte concentrations were as follows: 10 mM maltose, 10 mM fructose, 10 mM lactose, and 5 mM glucose. The error bars represent the standard deviation of three measurements. (B) The time-dependent absorbance changes at 652 nm for different samples (buffer solution or diluted blood samples) after incubation with GOx. Diluted blood was diluted 100-fold.

4. Conclusion

In summary, we successfully prepared Cu NPs/g-C_3N_4 via the calcination of dicyandiamide-Cu^{2+} complex with the assistance of humic acid. The prepared Cu NPs/g-C_3N_4 was found to have highly intrinsic peroxidase-like activity. Cu NPs/g-C_3N_4 could catalyze the oxidation of TMB by H_2O_2 to produce the typical blue color reaction. The catalytic activity was sensitive to variations of pH, temperature, catalyst amount, and substrate concentration. The Cu NPs/g-C_3N_4 catalyzed the reaction of H_2O_2 and TMB which showed typical Michaelis-Menton kinetics. A sensitive colorimetric method to detect H_2O_2 and glucose was developed by using Cu NPs/g-C_3N_4 peroxidase-like catalytic activity. The detection limits of H_2O_2 and glucose can be reached to 3.2×10^{-8} M and 3.7×10^{-7} M, respectively. This approach could be applied for glucose detection in real serum samples. As a novel peroxidase mimetic with highly sensitive property, Cu NPs/g-C_3N_4 would have potential applications in biocatalysts and clinical diagnosis.

Acknowledgements

This work was supported by the National Natural Science Foundation of China (Nos. 21375079, 51402175) and Project of Development of Science and Technology of Shandong Province, China (No. 2013GZX20109).

References

1 L. Gao, J. Zhuang, L. Nie, J. Zhang, Y. Zhang, N. Gu, T. Wang, J. Feng, D. Yang and S. Perrett, *Nat. Nanotechnol.*, 2007, 2, 577-583.
2 Y. Chen, H. Cao, W. Shi, H. Liu and Y. Huang, *Chem. Commun.*, 2013, 49, 5013-5015.
3 A. Asati, C. Kaittanis, S. Santra and J. M. Perez, *Anal. Chem.*, 2011, 83, 2547-2553.
4 Z. Wang, R. Lévy, D. G. Fernig and M. Brust, *J. Am. Chem. Soc.*, 2006, 128, 2214-2215.
5 Y. JuanáLong, Y. FangáLi, J. JiaáZheng and C. ZhiáHuang, *Chem. Commun.*, 2011, 47, 11939-11941.
6 K. Cai, Z. Lv, K. Chen, L. Huang, J. Wang, F. Shao, Y. Wang and H. Han, *Chem. Commun.*, 2013, 49, 6024-6026.
7 W. He, Y. Liu, J. Yuan, J.-J. Yin, X. Wu, X. Hu, K. Zhang, J. Liu, C. Chen and Y. Ji, *Biomaterials*, 2011, 32, 1139-1147.
8 T. Kwon, M. Min, H. Lee and B. J. Kim, *J. Mater. Chem.*, 2011, 21, 11956-11960.
9 C.-W. Lien, C.-C. Huang and H.-T. Chang, *Chem. Commun.*, 2012, 48, 7952-7954.
10 H. Chen, Y. Li, F. Zhang, G. Zhang and X. Fan, *J. Mater. Chem.*, 2011, 21, 17658-17661.
11 Z. Liu and Y. Bando, *Adv. Mater.*, 2003, 15, 303-305.
12 Z. Liu and Y. Bando, *Chem. Phys. Lett.*, 2003, 378, 85-88.
13 I. Lisiecki, H. Sack-Kongehl, K. Weiss, J. Urban and M.-P. Pileni, *Langmuir*, 2000, 16, 8807-8808.
14 I. Lisiecki, A. Filankembo, H. Sack-Kongehl, K. Weiss, M.-P. Pileni and J. Urban, *Phys. Rev. B*, 2000, 61, 4968-4974.
15 C. F. Monson and A. T. Woolley, *Nano Lett.*, 2003, 3, 359-363.
16 M. Y. Yen, C. W. Chiu, C. H. Hsia, F. R. Chen, J. J. Kai, C. Y. Lee and H. T. Chiu, *Adv. Mater.*, 2003, 15, 235-237.
17 H. Choi and S.-H. Park, *J. Am. Chem. Soc.*, 2004, 126, 6248-6249.

View Article Online
DOI: 10.1039/C5RA18957H

18 N. Goswami, A. Giri, M. Bootharaju, P. L. Xavier, T. Pradeep and S. K. Pal, *Anal. Chem.*, 2011, 83, 9676-9680.
19 X. Wang, S. Blechert and M. Antonietti, *ACS Catal.*, 2012, 2, 1596-1606.
20 J. Sun, J. Zhang, M. Zhang, M. Antonietti, X. Fu and X. Wang, *Nat. Comm.*, 2012, 1139, 1-6.
21 Y. Wang, J. Zhang, X. Wang, M. Antonietti and H. Li, *Angew. Chem. Int. Ed.*, 2010, 49, 3356-3359.
22 Y. Cui, Z. Ding, X. Fu and X. Wang, *Angew. Chem. Int. Ed.*, 2012, 51, 11814-11818.
23 E. Z. Lee, Y. S. Jun, W. H. Hong, A. Thomas and M. M. Jin, *Angew. Chem. Int. Ed.*, 2010, 49, 9706-9710.
24 Q. Xiang, J. Yu and M. Jaroniec, *Nanoscale*, 2011, 3, 3670-3678.
25 X. Chen, J. Zhang, X. Fu, M. Antonietti and X. Wang, *J. Am. Chem. Soc.*, 2009, 131, 11658-11659.
26 F. Goettmann, A. Thomas and M. Antonietti, *Angew. Chem. Int. Ed.*, 2007, 46, 2717-2720.
27 G. Liu, P. Niu, C. Sun, S. C. Smith, Z. Chen, G. Q. Lu and H.-M. Cheng, *J. Am. Chem. Soc.*, 2010, 132, 11642-11648.
28 J. Zhang, M. Zhang, C. Yang and X. Wang, *Adv. Mater.*, 2014.
29 J. Xu, L. Zhang, R. Shi and Y. Zhu, *J. Mater. Chem. A*, 2013, 1, 14766-14772.
30 X. Chen, X. Tian, B. Su, Z. Huang, X. Chen and M. Oyama, *Dalton Trans.*, 2014, 43, 7449-7454.
31 T. Lin, L. Zhong, J. Wang, L. Guo, H. Wu, Q. Guo, F. Fu and G. Chen, *Biosens. Bioelectron.*, 2014, 59, 89-93.
32 L. Hu, Y. Yuan, L. Zhang, J. Zhao, S. Majeed and G. Xu, *Anal. Chim. Acta*, 2013, 762, 83-86.
33 J. Tian, Q. Liu, A. M. Asiri, A. H. Qusti, A. O. Al-Youbi and X. Sun, *Nanoscale*, 2013, 5, 11604-11609.
34 L. Ge, C. Han, J. Liu and Y. Li, *Appl. Catal. A-Gen.*, 2011, 409, 215-222.